Thermal Science and Engineering Progress 71 (2026) 104559

Contents lists available at ScienceDirect

Thermal Science and Engineering Progress

journal homepage: www.sciencedirect.com/journal/thermal-science-and-engineering-progress

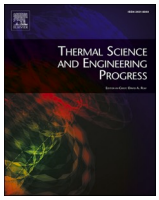

Lauric acid/refractory clay/expanded graphite composites for improved thermal energy storage characteristics

Yasemin Erben [a,1], Hatice Hande Mert [b,2,*], Mehmet Selçuk Mert [c,3]

[a] Yalova University, Institute of Graduate Studies, Chemical Engineering Department, Yalova 77200, Türkiye
[b] Yalova University, Faculty of Engineering, Chemical Engineering Department, Yalova 77200, Türkiye
[c] Yalova University, Faculty of Engineering, Energy Systems Engineering Department, Yalova 77200, Türkiye

ARTICLE INFO

Keywords:
Refractory clay
Phase change material
Thermal energy storage
Expanded graphite

ABSTRACT

Refractory clays (RC) are aluminosilicate based inorganic materials, which have unique properties such as low cost, high thermal stability, chemical resistance, mechanical strength and absorbability. In this study, RC, mainly composed of SiO_2 (56.01%), Al_2O_3 (41.96%) and TiO_2 (1.26%), was explored as a thermally stable and low-cost supporting material for development of LA based shape-stabilized composite PCMs, while expanded graphite (EP) was employed to develop heat transfer performance with maintaining shape stability. A series of LA/RC composites were prepared by solvent assisted impregnation method, and leakage tests were conducted to evaluate the shape-stabilization property. The morphological, chemical, thermal properties and phase change characteristics of the prepared composites were determined by scanning electronic microscope (SEM), Fourier transform infrared spectroscopy (FTIR), thermogravimetric analysis (TG) and differential scanning calorimetry (DSC). The maximum PCM weight fraction among the prepared composites was found to be 40 wt% without any leakage and this composite demonstrated good thermal reliability after repeated heating–cooling cycles. The latent heats and temperatures of the composite PCM were measured as 64.2 J/g and 43.46 °C for melting and 66.0 J/g and 41.77 °C for crystallization. The shape-stable composite PCM was modified with highly conductive EP particles with the aim of improving heat conduction property and eliminating drawbacks of low thermal conductivity due to RC support. The shape-stable LA/RC/EP composite displayed improved thermal conduction properties thanks to loading 5 wt% EP, while latent heats slightly decreased (63.6 J/g for melting and 61.7 J/g for crystallization) in comparison with undoped composite. LA/RC/EP composite is a promising energy material for passive energy storage applications such as solar energy storage and thermoregulation of buildings where shape stability and improved heat transfer are demanded under practical constraints.

1. Introduction

Using energy sources efficiently and providing continuity of energy supply is important factor for economic development of countries. In recent years, renewable energy as an alternative to conventional energy sources has gained increasing interest. Energy storage plays an important role in terms of efficient use of renewable energy resources, which are variable in nature, and in closing the energy supply–demand gap. Phase change material (PCM) has ability of storing and releasing latent heat during phase change at almost constant temperature [1–3]. Depending on their phase change characteristics, many different PCM types have the potential to be used in thermal energy storage systems. Among these, fatty acids are a member of organic PCM class have important place especially in passive solar thermal energy storage applications [4]. Fatty acids are carboxylic acids with long hydrocarbon chains and have many advantages such as being thermally stable, chemically stable, biodegradable, low cost and non-toxic [5–7]. Moreover, low corrosion activity and high melting enthalpy comparable to paraffins are prominent features of them. On the other hand, their low thermal conductivity and leakage problem that may occur due to their transition from solid to liquid phase restricts the direct use of these materials in energy storage systems [8–10]. Nowadays, the production

* Corresponding author.
E-mail address: hndmert@yalova.edu.tr (H.H. Mert).
[1] ORCID: https://orcid.org/0009-0007-2012-443X.
[2] ORCID: https://orcid.org/0000-0003-0743-1981.
[3] ORCID: https://orcid.org/0000-0002-8646-0133.

https://doi.org/10.1016/j.tsep.2026.104559
Received 21 July 2025; Received in revised form 7 January 2026; Accepted 3 February 2026
Available online 4 February 2026

of composite PCMs combined with a support material with high thermal conductivity has an increasing interest both in ensuring stability in shape and solving the leakage problem and in increasing thermal conductivity [11,12]. Researchers have focused on developing easy and inexpensive methods using various support materials for the production of shape-stable composite PCMs [13]. While the shape stability of PCMs can be achieved through the microencapsulation process in which organic or inorganic materials are used as shells, this feature can also be achieved by approaches using various porous materials (porous carbon, graphite, polyurethane foams, silica structures, clays) as support materials [14,15]. Clay minerals are frequently preferred in the preparation of shape-stable PCMs due to their excellent adsorption properties resulting from their porous structure. In addition, in research, materials with high thermal conductivity such as carbon nanotubes, graphene nanosheets and various metal or metal oxide additives are used to increase the heat transfer rates of organic PCMs [10]. Zhan et al. used graphene oxide (GO) as thermal conductivity enhancer to modify n-octadecane based microencapsulated PCMs and reported that the addition of GO led to a 55.8% increase in thermal conductivity [16]. Kumar et al. [10] designed composite PCMs consisting of gypsum/lauric acid/graphite components for the purpose of thermoregulation of indoor temperature in buildings and carried out the morphological and thermal characterization of the materials they obtained. It was observed that increasing the amount of graphite added in different proportions (0–10% by weight) increased the thermal conductivity of the materials and decreased their thermal energy storage capacity from 81.08 J/g to 54.30 J/g. As a result of the thermal cycling test (1000 cycles), it was concluded that the thermophysical properties of all the materials obtained were preserved and they were thermally reliable. Liu et al. [9] prepared a eutectic mixture with fatty acid-based PCMs, lauric acid and stearic acid, and produced form-stable PCMs using expanded perlite as a support material. The melting temperature of the composite material was found to be 37.79 °C and the melting enthalpy was 126.05 J/g, and the material displayed good thermal stability. In another study using lauric acid and bentonite components, carbon nanofibers were used to improve the thermal conductivity [17]. Researchers found that 5% carbon nanofiber addition increased the thermal conductivity of the composite by two times. Liu et al. [18] used six different clay minerals (attapulgite, sepiolite, vermiculite, diatomite, bentonite and kaolin) as support matrix for the shape stabilization of capric acid-palmitic acid binary eutectic PCM and compared the morphological, chemical and thermal properties of the composites obtained. The results showed that all six composite PCMs had good thermal stability, while sepiolite exhibited the worst adsorption capacity. A hybrid PV cooling system combining PCM, and clay based evaporative cooling was investigated based on mathematical modeling by Ali et al. [19]. Modeling results have shown that PV/clay cooling system demonstrated higher performance than other cooling methods whereas the hybrid PV-PCM/clay system has been identified as the most economically advantageous option, especially at low rear-surface coverage. The thermal and mechanical effects of adding commercially available microencapsulated PCMs (mPCMs) to silty clay at different ratios were investigated [20]. In general, it has been reported to mPCM improved the thermal properties of silty clay, and lower doses are usually appropriate for optimum mechanical performance. In another work, mPCMs were used to prevent cracking in silty clay and to determine the deformation and strength characteristics of samples included mPCM at different ratio were tested [21]. It has been reported that silty clay containing 2% mPCM has demonstrated increased shear strength and reduced cracking and deformation.

Even though kaolinite and bentonite are conventional clay materials with layered aluminosilicates widely used as supporting material for shape-stabilization of PCM [22], some structural changes due to dehydroxylation and structural collapse of the crystalline structure at moderately elevated temperatures [23] may cause limitations such as relatively low structural robustness and thermal endurance under extended thermal cycling and elevated temperatures. This situation can adversely affect shape stability, latent heat storage, and thermal-cycling reliability.

Refractory clays (RC) are extensively used inorganic materials in many areas associated with metallurgical industries, which have high temperature resistance, chemical stability, and heterogeneous microstructure. RC serves a fundamentally different structural and thermal characteristics from conventional clay materials with thanks to possessing thermally stable, rigid, non-swelling porous network, higher alumina content, which physically stabilizes the PCM and maintains its structural integrity and pore architecture over repeated heating–cooling cycles. This structure offers advantages such as increased thermal reliability, reduced risk of leakage, and more stable latent heat performance during prolonged thermal cycling.

RC takes part in kaolinite groups, which consists of aluminum silicate structure [24]. Even RC mainly composed of alumina (Al_2O_3) and silica (SiO_2), specific composition varies depending on the source of the clay. Although its remarkable thermal stability, chemical resistance, and mechanical strength make RC a potential support material for shape stabilization of PCM, its main disadvantage is its low thermal conductivity.

In this study, it is aimed to eliminate the disadvantages of leakage and low thermal conductivity of during application, to ensure chemical and thermal stability, and to obtain energy-storing composites with high thermal energy storage capacity. To our knowledge, RC has not been systematically investigated before as a supporting matrix for PCM with respect to structural rigidity and thermal endurance. This unique structure of RC combining high temperature stability and pore integrity constitutes the main novelty of the present study. In this regard, this study was focused on the production and characterization of economical, form-stable, chemically and thermally reliable lauric acid (LA)/refractory clay (RC) composites that can be used for solar energy storage applications. The maximum LA absorption capacity in RC was determined by conducting a series of experiments and the obtained composites were fully characterized in terms of chemical, morphological, and thermal energy storage properties. The heat conduction properties of the shape-stable composite PCM with the highest heat storage capacity were improved by modification with highly conductive expanded graphite particles. In addition to revealing the usability of refractory clay as a support matrix in shape stabilization, this study is thought to have potential applications in solar heat storage and contribute to the development of new composite PCMs.

2. Experimental section

2.1. Materials

Refractory clay (RC) was kindly supplied from commercial firm (Ferroser, Türkiye) and lauric acid (LA, ≥98%, $C_{12}H_{24}O_2$, MW = 200.32 $g.mol^{-1}$, melting point:44–46 °C) purchased from Sigma-Aldrich. Expanded graphite (EP, highly conductive, micron powder, purity 96+%, size 70 μm) was bought from Nanografi, Türkiye. Ethanol and acetone were received from Merck (Darmstadt, Germany) and used as carrier solvents. All the chemicals in the experiments were used as supplied. RC was treated thermally at 105 °C for 24 h in a vacuum oven to remove physically adsorbed moisture.

The chemical composition of RC was determined by X-ray Fluorescence spectroscopy and presented in Table 1. As seen from Table 1, the major components available in RC are SiO_2 (56.01%), Al_2O_3 (41.96%) and TiO_2 (1.26%).

2.2. Preparation of LA/RC composites

LA/RC composites were prepared by the solvent assisted impregnation process based on the PCM/support material composition ratio listed in Table 2 using a fixed total composite mass of 1 g. First, LA was heated

Table 1
Chemical composition of RC obtained by the X-ray Fluorescence (XRF).

Element Form Symbol	Element	Concentration (ppm)	Oxide Form Symbol	Element	Concentration (wt.%)
Si	Silicon	261,800	SiO_2	Silicon	56.01
Al	Aluminum	222,100	Al_2O_3	Aluminum	41.96
K	Potassium	8911	TiO_2	Titanium	1.26
Ti	Titanium	7565	K_2O	Potassium	1.07
Fe	Iron	5917	Fe_2O_3	Iron	0.84
Na	Sodium	5770	Na_2O	Sodium	0.77
Mg	Magnesium	2625	MgO	Magnesium	0.43
Ca	Calcium	2179	CaO	Calcium	0.30
S	Sulfur	408.9	SO_3	Sulfur	0.10
P	Phosphorus	296.3	P_2O_5	Phosphorus	0.06

Table 2
The composition ratio of LA/RC composite PCMs.

Sample Name	Composition Ratio (wt.%)	Leakage behavior
LA/RC-2575	25%LA-75%RC	No leakage
LA/RC-3070	30%LA-70%RC	No leakage
LA/RC-3565	35%LA-65%RC	No leakage
LA/RC-4060	40%LA-60%RC	No leakage
LA/RC-4555	45%LA-55%RC	Leakage

above its melting point and dispersed in ethanol as the carrier solvent at a composite-to-solvent ratio of 1:100 (w/v). Then, RC was added, and the solution placed in an ultrasonic bath for homogenization for 30 min at 55 °C. After that, the solution was mechanically stirred at 55 °C for 24 h and placed in vacuum oven at 65 °C. After solvent was removed, the powder LA/RC composites were obtained. In the next step, leakage test was performed to determine the stable composite PCM containing maximum LA. In this aim, certain amounts of LA/RC composite PCMs at different compositions were put on the blue band filter paper (diameter: 125 mm) with a circle (diameter: 25 mm) drawn and placed on a plate in an oven preheated to 65 °C. After 2 h, the samples were evaluated for any leakage. The composites without visible oily spot on the filter paper were evaluated as leak-proof. The test results are given in Table 2, and the photographs of the samples taken after the test are presented in Fig. 1. As depicted in Fig. 1, LA was stable at room temperature, whereas it melted and transformed into liquid form at the end of the test. On the other hand, the composite PCMs preserved their shape-stability, and no leakage trace was detected on the filter paper other than that's of the LA/RC-4555 composite. According to this result, LA/RC-4060 is the shape-stabilized composite that holds maximum LA without any leakage.

As improving thermal conductivity of LA/RC composites, *LA/RC-4060* were doped with highly conductive expanded graphite (EP) particles. EP particles (5 wt% regarding the total amount of LA/RC composite) were dispersed in acetone and put on an ultrasonic bath preheated to 35 °C for homogenization. The composite PCM was added onto EP solution and stirred mechanically at 400 rpm for 30 min. The resultant solution was placed in a vacuum oven at 35 °C and the solvent was removed. The obtained final composite was called as *LA/RC-4060–5%EP*. The production steps of composite PCMs prepared at different LA and RC compositions (wt.%) were given in Fig. 2.

2.3. Characterization

The chemical composition of RC was determined by X-ray Fluorescence spectroscopy (XRF, Spectro, Xepos II). Morphologic and chemical structure analyses of the samples were performed by scanning electron microscopy (SEM, FEI, Quanta FEG 250), which operated at an accelerating voltage of 5–20 kV and Fourier transform infrared spectroscopy (FTIR) (Perkin Elmer, Spectrum 100) recorded in the range of 4000–600 cm^{-1} at 4 cm^{-1} resolution, respectively. The phase transition temperatures and latent heat of melting/crystallization of the composites were determined by differential scanning calorimetry (Perkin Elmer DSC 4000). The measurements were conducted under an inert N_2 atmosphere between temperature ranges of 0 to 80 °C with a 10 °C.min^{-1} heating/cooling rate. The thermal stabilities of the composites were investigated by thermogravimetric (TG) analysis (TGA, HITACHI, STA 7300) at a heating rate of 10 °C.min^{-1} between 25 – 600 °C temperature range under inert N_2 medium with a gas flow rate of 50 mL.min^{-1}. In addition, specific surface area and pore characteristics of RC before and after impregnation of LA were determined based on the Brunauer–Emmet–-Teller (BET) adsorption model by Micromeritics Gemini VII 2390 t Fully Automatic BET Instrument. Before the measurement, samples were degassed at 100 °C for 24 h in Micromeritics FlowPrep 060 Sample

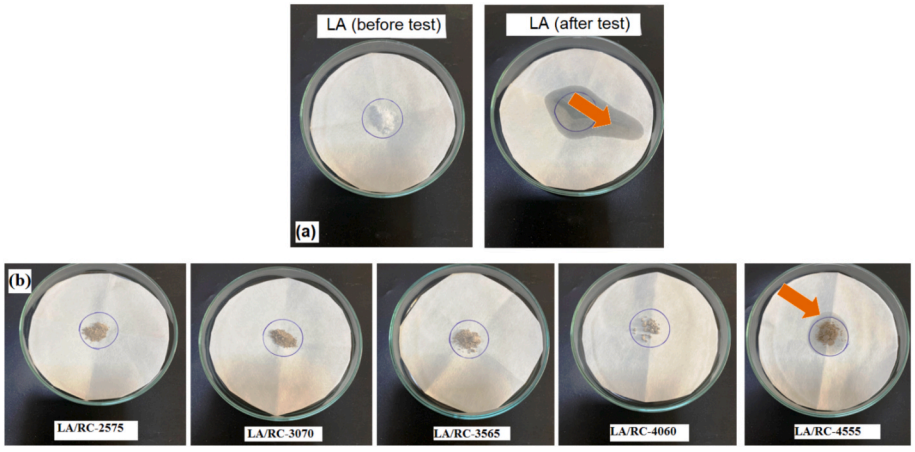

Fig. 1. Results of leakage test (a) LA and (b) LA/RC composite PCMs.

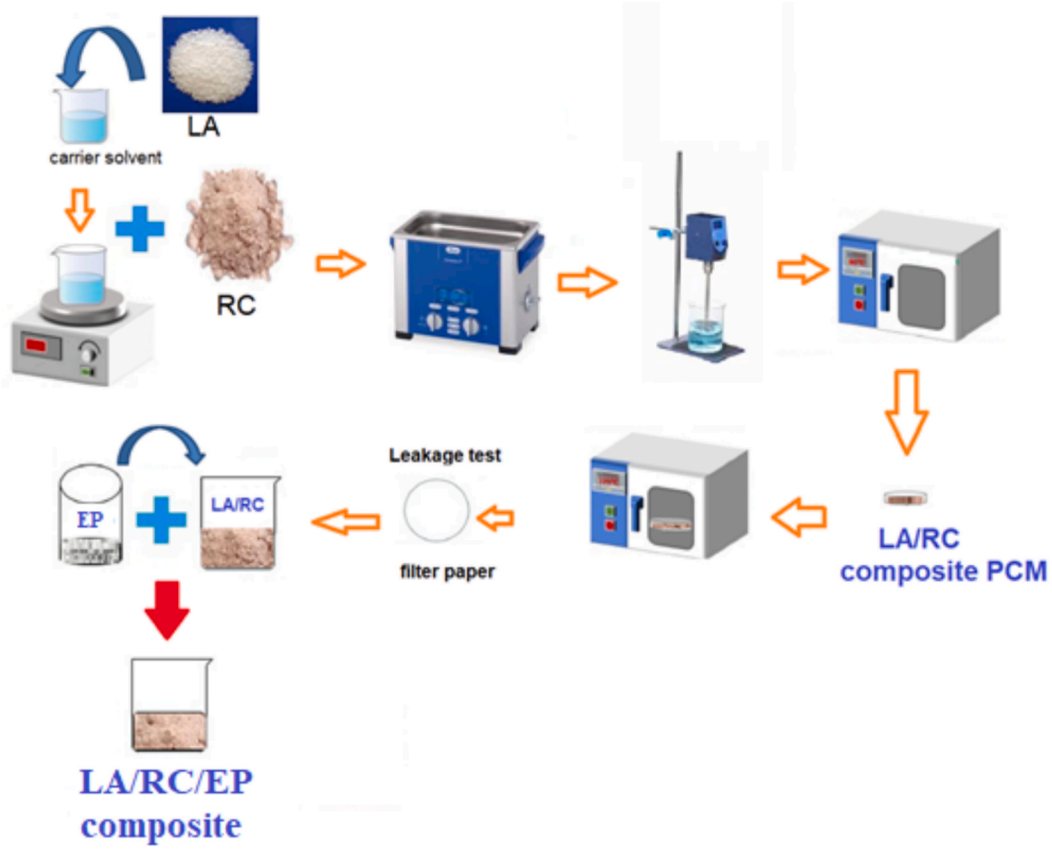

Fig. 2. Preparation steps of LA/RC and LA/RC/EP composite PCMs.

Degas System. Ruicheng MTC 3200 Instrument used for testing thermal reliability of the composite PCM and 100 sequential heating/cooling cycles were realized between the 10 °C – 80 °C. The thermal behavior of the samples was monitored by applying the T-history test with an experimental setup established at laboratory scale.

3. Results and discussion

3.1. Characterization of RC and LA/RC composite PCMs

3.1.1. Morphological analysis results

Fig. 3 demonstrates the microstructure of RC and LA/RC composites (LA/RC-2575, LA/RC-3070, LA/RC-3565 and LA/RC-4060). As clearly seen from Fig. 3a, RC consists of stacked layered particles and irregular pores. On the other hand, it is noticed in SEM images of LA/RC composites that it covers the surfaces with increasing LA ratio. As seen in Fig. 3(b) – 3(e), LA spreads on the RC surface and pores as a layer of flake by adhering with thanks to capillary and surface tension forces.

3.1.2. Chemical analysis results

The chemical structure of RC, LA and LA based composite PCMs were investigated by FT-IR and obtained spectra were depicted in Fig. 4a and 4b. In the spectrum of LA (Fig. 4a), the asymmetric and symmetric stretching vibrations of methylene groups were aroused as the

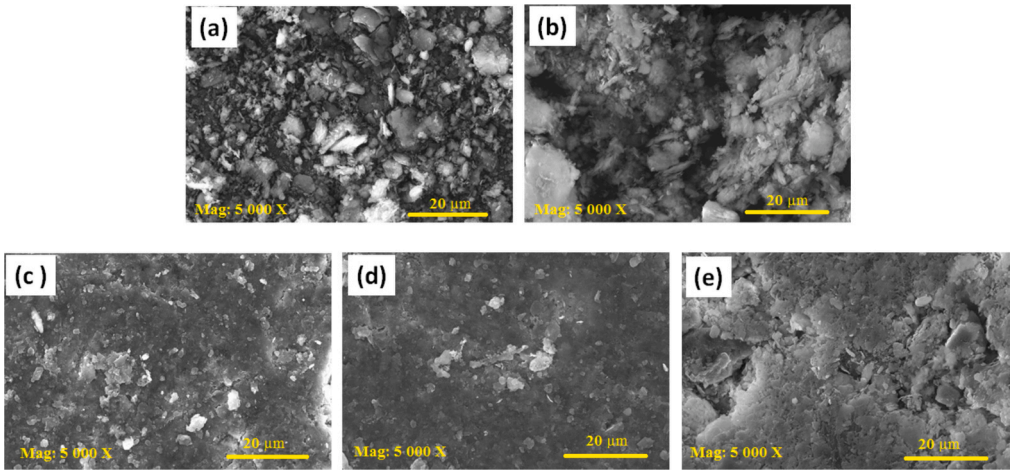

Fig. 3. SEM images (5000 x magnifications) of (a) RC, (b) LA/RC-2575, (c)LA/RC-3070, (d) LA/RC-3565, (e) LA/RC-4060.

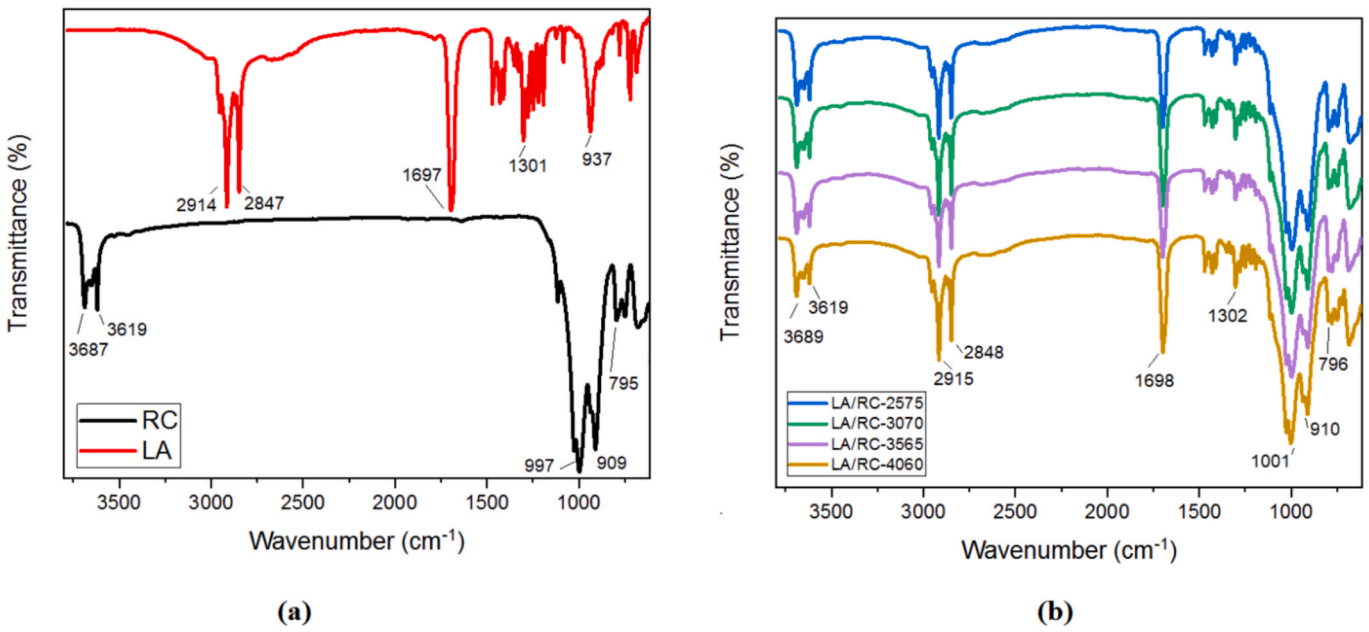

Fig. 4. FTIR spectra of (a) RC and LA, (b) LA/RC composite PCMs.

absorption peaks at 2914 and 2847 cm^{-1} [4,25]. The absorption band detected at 1697 cm^{-1} is characteristics for fatty acids and corresponds to stretching vibration of C=O group [26,27]. In RC spectrum, the bands located at 3687 cm^{-1} and 3619 cm^{-1} could be assigned to hydroxyl groups (OH) of RC, while the other bands aroused at 1100–997 cm^{-1} due to Si-O bonds [28]. The absorption band at 909 cm^{-1} could be attributed to Al-OH deformation vibration [28,29]. The double peaks located at 795 and 749 cm^{-1} are due to quartz vibrations corresponding to Si-O and Si-O-Al vibrations [28,29].

The presence of characteristic peaks of LA and no arouse of any new peaks in spectra of composite PCMs refers to absence of any chemical reaction between LA and RC. This result verified that absorption of LA into pores of RC was realized by physical interaction, and form stabilization of LA with RC was accomplished.

3.1.3. Thermal energy storage characteristics of LA and LA based composite PCMs

The phase change behavior and thermal energy storage characteristics of LA and composite PCMs were analyzed by DSC. The heating and cooling curves and corresponding data provided by DSC were presented in Fig. 5 and Table 3. As can be clearly seen from the phase transition curves, the composite PCMs displayed similar phase change characteristics with those of the LA, which verified the ability of the composites to store thermal energy as latent heat. This also serves as a marker of the absence of chemical reaction between RC supporting material and LA. The latent heats of melting and crystallization of LA measured as 176.5 J/g and 180.9 J/g, while onset melting and crystallization temperatures assigned as 44.67 °C and 40.86 °C, respectively. On the other hand, latent heats of melting and crystallization of the composite PCMs were detected as 39.3 J/g and 37.6 J/g for LA/RC-2575; 52.0 J/g and 50.7 J/g for LA/RC-3070; 52.7 J/g and 52.2 J/g for LA/RC-3565, and 64.2 J/g and 66.0 J/g for LA/RC-4060. In addition, onset melting and crystallization temperatures slightly displaced owing to the restriction of LA in a porous supporting material. As can be noticed from Table 3, latent heat of melting value increased relatively with the increased LA portion in the composites. Moreover, based on the values of incorporation ratio (R) incorporation efficiency (E), and thermal storage capability (η) calculated according to the equations in the literature [2,30,31], it was

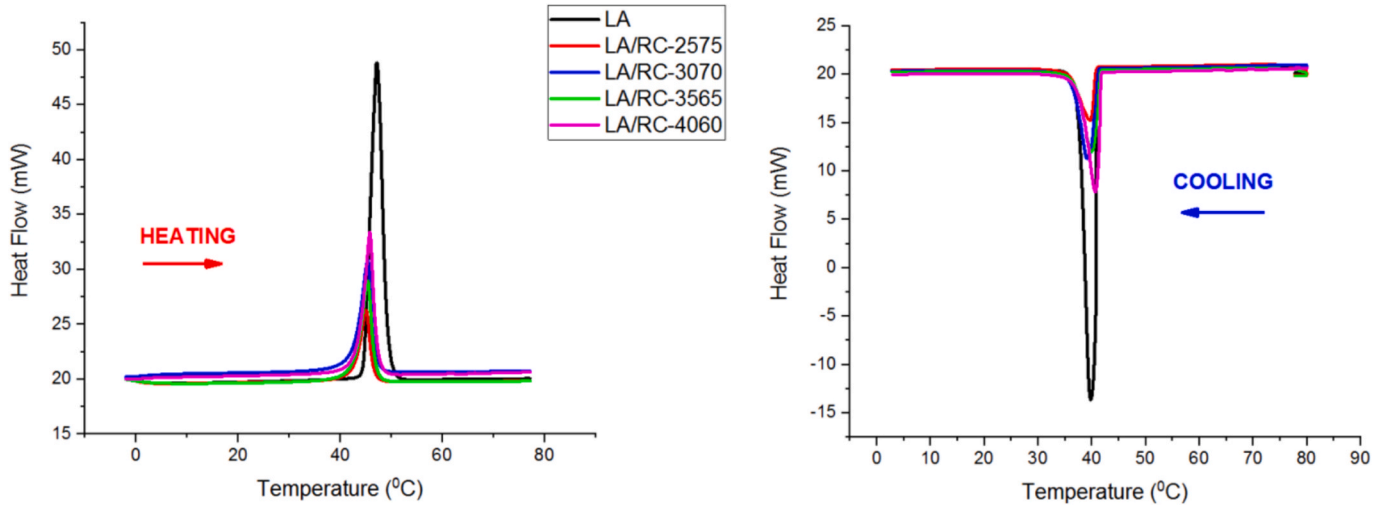

Fig. 5. DSC curves of LA and composite PCMs during heating and cooling.

Table 3
DSC analysis data of LA and LA/RC composite PCMs.

Samples	During Heating				During Cooling				R (%)	E (%)	η (%)
	[a]T_{om} (°C)	[b]T_{pm} (°C)	[c]T_{em} (°C)	[d]ΔH_m (J.g^{-1})	[e]T_{oc} (°C)	[f]T_{pc} (°C)	[g]T_{ec} (°C)	[h]ΔH_c (J.g^{-1})			
LA	44.67	47.25	49.18	176.5	40.86	39.80	37.78	−180.9	–	–	–
LA/RC-2575	42.77	45.02	46.54	39.3	40.79	39.73	36.25	−37.6	22.26	21.52	96.66
LA/RC-3070	42.67	45.45	46.89	52.0	41.23	39.15	36.64	−50.7	29.46	28.73	97.54
LA/RC-3565	42.87	45.32	46.88	52.7	41.54	39.96	36.77	−52.2	29.85	29.35	98.33
LA/RC-4060	43.46	45.80	47.23	64.2	41.77	40.70	37.89	−66.0	36.37	36.43	100

[a] *onset melting temperature.*
[b] *peak melting temperature.*
[c] *endset melting temperature.*
[d] *latent heat of melting.*
[e] *onset crystallization temperature.*
[f] *peak crystallization temperature.*
[g] *endset crystallization temperature.*
[h] *latent heat of crystallization*

determined that LA/RC composite PCMs have thermal storage capability of over 96%. The LA/RC-4060 composite is a prominent energy material among the produced composites, which has the highest melting enthalpy value without any seepage. It also had the highest integration ratio (R) and integration efficiency (E), which resulted in 100% thermal storage capacity calculated by dividing (E) to (R). According to this result, LA/RC-4060 composite has the potential to be utilized for applications such as solar energy storage, building thermal management with its proper energy storage characteristic.

3.1.4. Thermogravimetric analysis results

Thermal stability is a crucial property for PCMs in terms of thermal storage applications. Thermal stability of the produced composite PCM (LA/RC-4060) was investigated and the obtained TG thermogram depicted in Fig. 6 together with those of LA and RC comparatively. As can be seen from Fig. 6, LA has one degradation step. It was found that LA lost 50% of its weight at 212.0 °C and the peak maximum temperature value (T_{max}) with the highest weight loss was 225.68 °C. The total mass loss of LA at 550 °C was determined as 98.04%. The RC as host material was also degraded in one step due to dehydroxylation and the highest weight loss was detected at 505.22 °C. The total mass loss of RC at 550 °C was measured as 8.62%. Moreover, the composite PCM degraded in two steps. In the first step, the thermal decomposition of LA occurred nearly at 226.4 °C and the second step, dehydroxylation of RC at 505.06 °C. The composite PCM lost 10% and 30% of its mass at

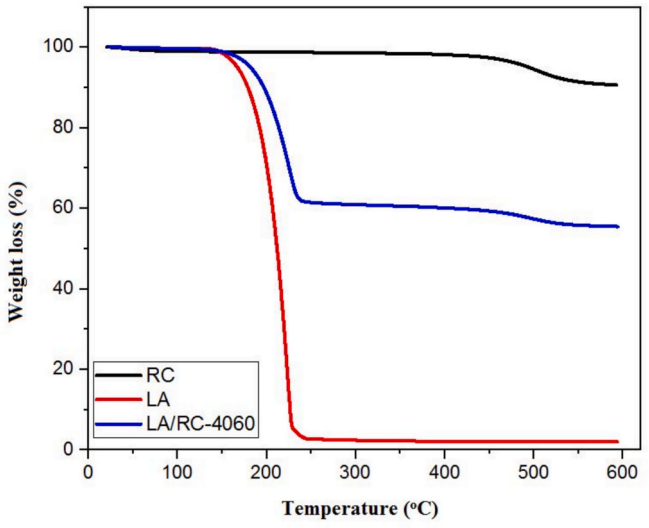

Fig. 6. TG curves of LA, RC and LA based composite PCM.

197.07 and 225.56 °C, respectively while these values were determined as 179.14 and 200.72 °C for pure LA. According to this result, it is obvious that RC has retarded the volatility of organic molecules. As shown in Fig. 6, thermal degradation temperature of LA shifted to higher temperature thanks to shape stabilization with RC.

The specific surface area and pore volume of RC and LA/RC-4060 were detected by BET analysis and obtained results presented in Table 4. Moreover, N_2 adsorption–desorption isotherms, and pore size distribution plot of RC are depicted in Fig. 7a and 7b, respectively. As seen from Fig. 7a, RC has adsorption capacity of 74.16 cm^3.g^{-1} at p/p^0 = 0.99 while it was measured as 4.17 cm^3.g^{-1} at lower relative pressure (p/p^0 = 0.05). The specific surface area according to BET method and pore volume of RC based on BJH adsorption model were determined as 20.08 m^2.g^{-1} and 0.1156 cm^3.g^{-1}, respectively.

This result demonstrates that RC has an adequate potential for absorbability of LA. Moreover, BJH adsorption average pore width (4 V/A) of RC was determined as 22.12 nm indicating a pore system dominated by mesopores. After the impregnation of LA and production of composite PCM, the specific surface area and pore volume of RC decreased dramatically and were found to be 1.65 m^2.g^{-1} and 0.0121 cm^3.g^{-1}, respectively. This is an expected result that is due to LA occupying the pores and layers of the RC. Pores in this size limit the accessible pore volume available for complete PCM impregnation, which explains the relatively moderate maximum LA loading capacity (40 wt%) observed. However, such mesoporous structures generate strong capillary forces that effectively restrict the PCM within the support matrix, preventing leakage during the phase transition [32].

Thermal reliability is an important parameter for thermal energy storage and should be taken into account in case of potential application of energy storage materials. For this purpose, LA/RC-4060 composite with the highest energy storage capacity was assessed by thermal cycling test. The acquired DSC curves of the LA/RC-4060 composite before and after 100 heating/cooling cycles were depicted in Fig. 8 and corresponding data was given in Table 5. As seen in Table 5, the latent heats of melting and crystallization of the composite after cycling test decrease by only 3.4 J/g and 3.6 J/g, respectively. The losses observed in melting and crystallization enthalpies were found to be 5.3% and 5.5%, respectively. Furthermore, the deviation in peak temperatures was found to be 0.65 °C for melting and 0.55 °C for crystallization after 100 thermal cycles. Based on the results, LA/RC-4060 composite has

Table 4
BET results of RC and composite PCM.

Samples	Specific surface area (m^2.g^{-1})	Pore volume (cm^3.g^{-1})
RC	20.08	0.1156
LA/RC-4060	1.65	0.0121

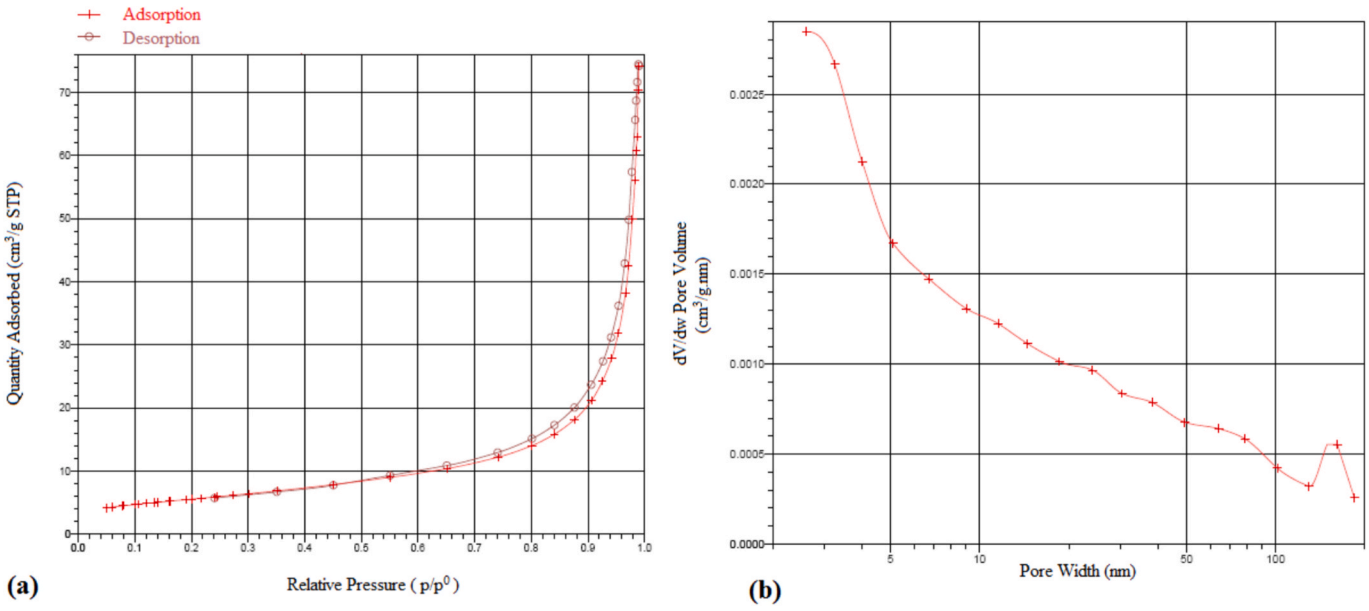

Fig. 7. (a) N_2 Adsorption-desorption isotherms of RC, and (b) pore size distribution plot of RC according to BJH method.

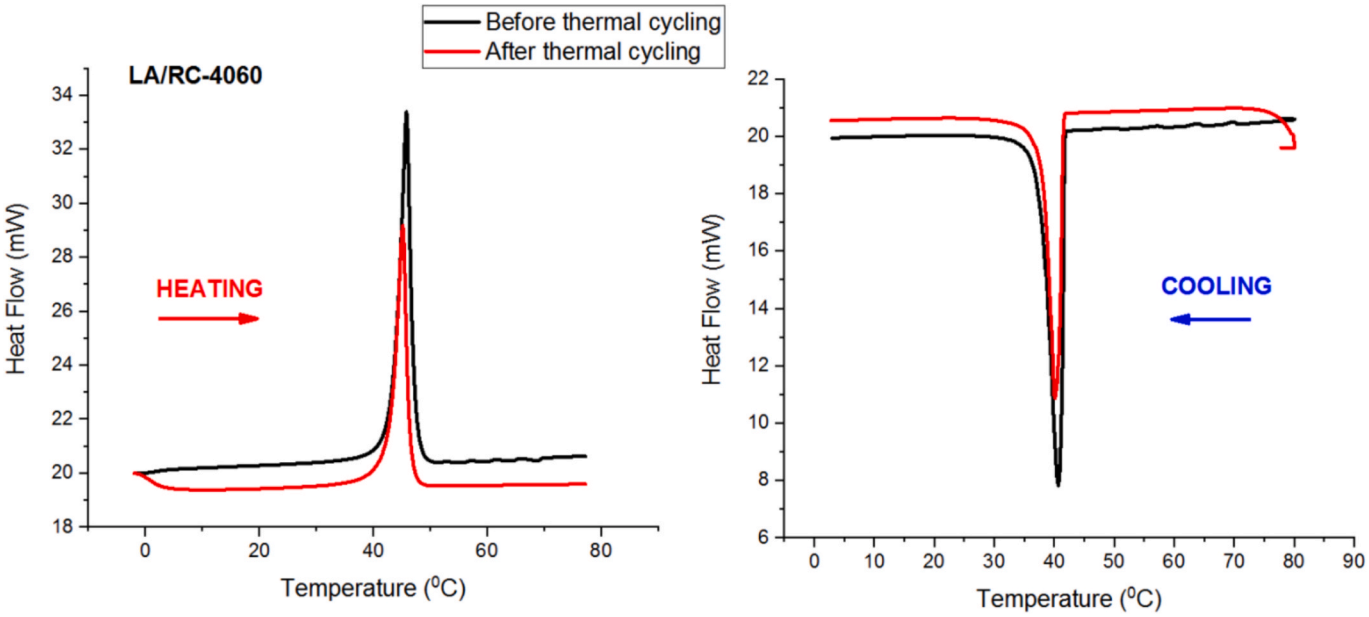

Fig. 8. Comparative DSC curves of LA/RC composite obtained before and after thermal cycling test.

Table 5
DSC data for LA/RC-4060 composite before the test and after 100th thermal cycle.

LA /RC-4060 composite	Melting		Crystallization	
	T_{pm} (°C)	ΔH_m (J.g^{-1})	T_{pc} (°C)	ΔH_c (J.g^{-1})
Before the test	45.80	64.2	40.70	−66.0
After 100th thermal cycle	45.15	60.8	40.15	−62.4

good thermal reliability, which is reasonable for potential applications.

3.1.5. Characterization and heat storage performance of EP loaded composite

The chemical structure of modified composite by EP was analyzed by FT-IR spectroscopy and the obtained spectra are given comparatively in Fig. 9. As noticed from the Fig. 9, EP has not any significant peak due to being chemically inert. In the case of LA/RC-4060–5%EP composite, although intensity of the peaks slightly decreased, any shift in absorption peaks was not observed as compared to that of LA/RC-4060 composite. According to the results, there is no chemical reaction due to the presence of EP, and the modification was achieved only physically.

The morphology of LA, EP, LA/RC-4060 and LA/RC-4060–5%EP were investigated by SEM and obtained images are depicted in Fig. 10. As seen from the SEM image of the LA/RC-4060 composite (Fig. 10c), the RC surface was covered with LA of the form of flaky layers (Fig. 10a), while highly conductive EP structures in the form of smooth layers (Fig. 10b) were seen also incorporated into the surface after modification (Fig. 10d).

The TGA thermograms remarking of the thermal stability of the

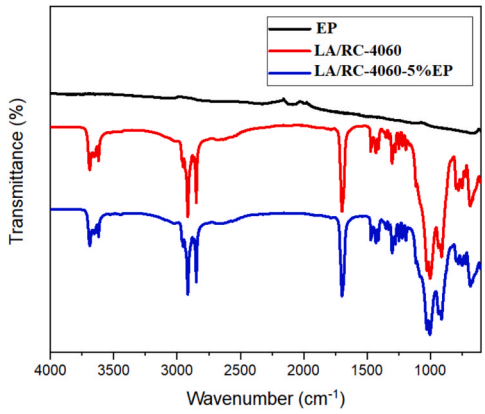

Fig. 9. FT-IR spectra of EP and EP loaded composite PCM.

modified composite by EP are presented in Fig. 11 as before and after modification for comparison. As seen from the thermograms, the modified composite degraded in two steps similarly as before the modification depending on high thermal stability of EP particles. Although thermal decomposition in the first step corresponding to degradation of organic PCM realizes earlier in comparison with that of the unmodified composite, the observed total mass loss is lower after the modification with EP particles. The total mass loss for modified composite LA/RC-4060–5%EP was found to be as 44.23% at 550 °C. Moreover, the maximum peak temperature values (T_{max1} and T_{max2}) with the highest weight losses were determined as 201.67 °C and 496.15 °C, respectively, which are significantly higher than the phase change temperatures as similarly observed for LA/RC-4060 composite. So, it is evident that both of the composites have good thermal stability and could be used confidently in thermal storage applications agreeable with their phase change temperatures.

The variation on the phase change characteristics of EP loaded composite PCM was investigated by DSC analysis and DSC thermograms obtained during heating and cooling are given in Fig. 12. As can be noticed from the thermograms, the presence of EP did not disturb the phase change property and EP loaded composite PCM displayed similar phase change properties with LA and LA/RC-4060 composite. The latent heat of composite LA/RC-4060–5%EP was found to be 63.6 J/g for melting and 61.7 J/g for crystallization. Furthermore, phase change temperatures were slightly changed due to the presence of highly conductive EP particles. The comparison of LA/RC-4060 and LA/RC-4060–5%EP composites with other fatty acid-based shape-stabilized PCMs available in the literature is demonstrated in Table 6. As can be clearly seen, the prepared composites have relatively high latent heat of melting values. Based on this data, it could be remarked that the obtained shape-stabilized composites are prospective energy materials for energy storage applications such as solar energy storage, thermoregulation of buildings.

Thermal conduction property is a significant indicator of heat transfer rate of PCM and is a crucial character that must be taken into consideration for TES applications of PCMs [33]. Here, thermal behavior of the samples, namely, EP, RC, LA/RC-4060, LA/RC-4060–5%EP and LA were evaluated by T-history test during heating and cooling steps. For this aim, an experimental test rig was set up including a circulated − bath, data acquisition system and K-type thermocouples with an uncertainty of ± 0.75%. The samples were equivalently (~1 g) placed in the cylindrical test tubes made of glass, with an inner diameter of 12 mm and a height of 75 mm to eliminate the geometric differences. Subsequently, K-type thermocouples were installed in the midpoint of the tubes to mitigate the effect of axial and radial temperature gradients during the temperature measurements of the samples. Afterwards, the tubes were immersed in the circulated − bath, which has an internal pump providing the homogenous temperature distribution within it. The circulated − bath was adjusted to operate in the temperature range of 25 °C – 60 °C – 25 °C. When the samples reached the initial temperature at 25 °C, the test was started and the temperature changes of the samples were measured with the installed thermocouples and collected at 1 s intervals with the data acquisition system. To monitor the original phase and/or temperature change of the samples, raw temperature–time data were plotted as obtained, without any processing. Fig. 13 shows the temperature measurements indicating the thermal behavior of the samples comparatively based on the conducted T-history test. As seen from the Fig. 13, the phase transition process of the samples LA, LA/RC-4060 and LA/RC-4060–5%EP was clearly observed during both heating and cooling steps. Based on the examinations, it was revealed that the findings of the T-history test consistent with the data obtained from DSC analyses (Table 3). On the other hand, EP and RC did not give phase

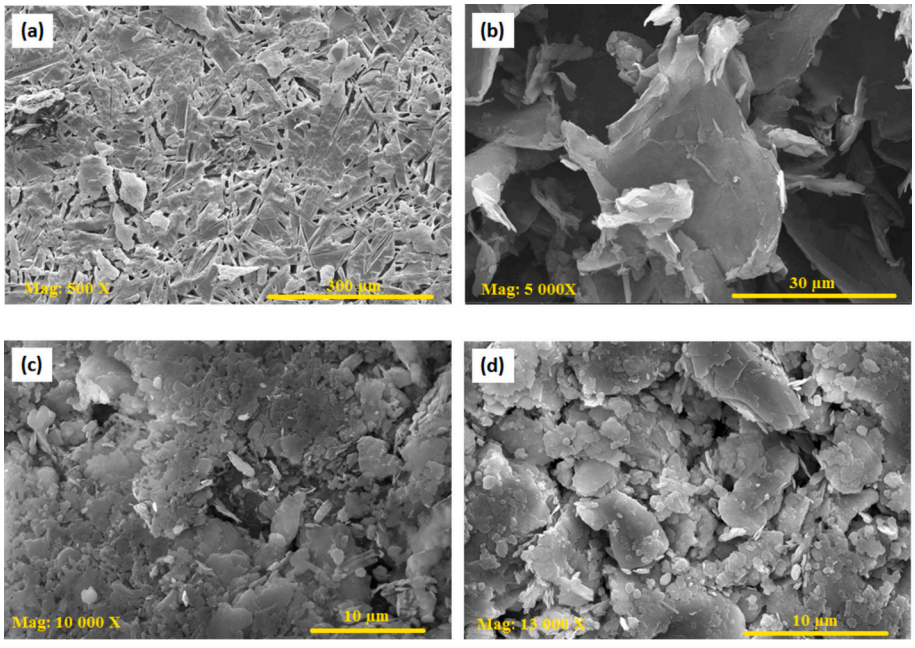

Fig. 10. SEM images of (a) LA, (b) EP, (c) LA/RC-4060 and (d) LA/RC-4060–5%EP.

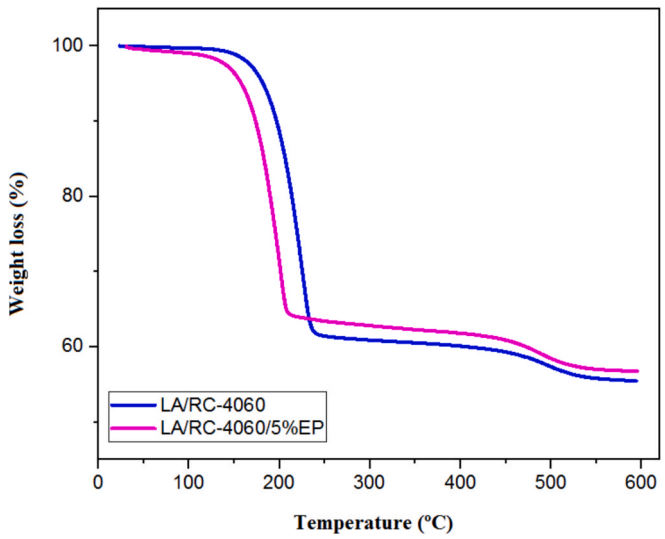

Fig. 11. TG thermograms of composite LA based composite PCM before and after EP loading.

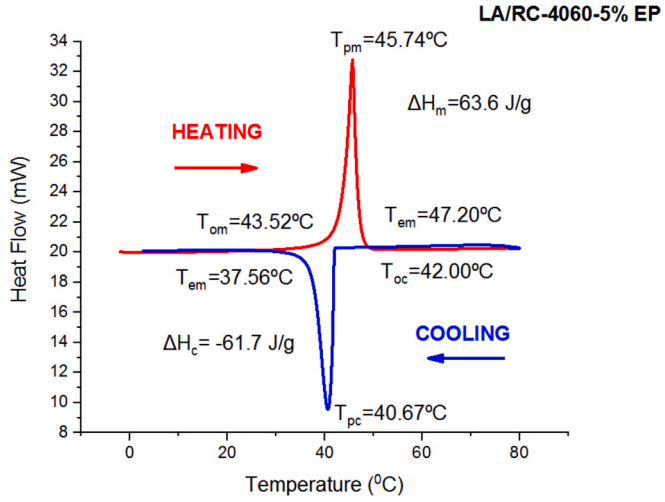

Fig. 12. DSC thermograms of EP loaded composite PCM during heating and cooling presented with phase transition data.

Table 6
Comparison of LA based PCMs in the literature.

LA integrated composite	Tm	ΔH_m (J.g^{-1})	Reference
Lauric-Myristic-Palmitic acid/ Diatomite	29.8	65.8	[5]
Gypsum/Lauric acid-graphite-zeolite	42.0–45.7	54.3–81.0	[10]
Capric-lauric acid/ Coal-series kaolinite	16.9	42.3	[35]
Lauric acid/raw fly ash	45.7	44.9	[36]
Lauric acid/raw fly ash/carbon nanotube	45.3	37.8	[36]
Lauric acid-myristic acid/fly ash	31.1	45.3	[37]
Lauric acid/nano-Cu/attapulgite	42.1	87.1	[38]
LA/RC-4060	43.4	64.2	This study
LA/RC-4060–5%EP	43.5	63.6	This study

transition peaks because they did not have energy storage capability. In addition, the heat conduction properties of the samples were compared by taking into account the time required to reach a target temperature. The shorter melting/crystallization times indicates an increased charging/discharging rate which is due to improvement in thermal conductivity [34]. As clearly demonstrated in the cooling step, EP was first reached the target temperature (from 60 °C to 25 °C) as expected since it was highly conductive expanded graphite. Additionally, when the heat transfer rates of the all samples were compared depending on the time to reach the target temperature, it was seen that the heat conduction properties were in the order of EP > RC > LA/RC-4060–5% EP > LA/RC-4060 > LA. As can be noticed from Fig. 13, longer charging/discharging times of LA was shortened after shape-stabilization by RC support due to probable higher thermal conductivity of RC than that of fatty acid PCM. Furthermore, since LA/RC-4060–5%EP > LA/RC-4060 > LA, it was clearly observed that even incorporating only 5 wt% EP in the structure significantly improved the heat transfer rate of the LA/RC-4060 composite PCM due to betterment in thermal conductivity. Moreover, in order to express these findings numerically, a property defined as the heat storage rate, calculated by dividing the specific temperature difference by the time to reach the target temperature, was determined for all samples and is given in Table 7. According to the results obtained, the calculated heat storage rates were also in the order of EP > RC > LA/RC-4060–5%EP > LA/RC-4060 > LA. The improvements in heat conduction rate during cooling process in comparison with that of LA were calculated as 13.66% for LA/RC-4060 and 15.85% for LA/RC-4060–5%EP.

4. Conclusions

This study focuses on investigating the availability of RC, which possesses economic and environmental advantages such as low cost, natural abundance, and chemical stability, as a thermally stable and structurally supporting matrix for the shape stabilization of PCMs. The shape-stabilized lauric acid (LA)/refractory clay (RC) composites were successfully prepared by the solvent assisted impregnation process. RC, mainly composed of SiO_2 Al_2O_3 and TiO_2 components, was used as the support material, whereas lauric acid used as the organic based PCM. A series of LA/RC composite PCMs at different compositions were synthesized. LA/RC-4060 composite was detected as the leak-proof composite with maximum LA loading capacity based on the conducted leakage test, which has 40%LA-60%RC composition. The thermal energy storage characteristics of LA and composite PCMs were detected by DSC, and the morphologies were elucidated by SEM analysis. The physical absorption of LA into pores of RC was demonstrated by SEM images, and the chemical structure investigated by FTIR spectroscopy proved the existence of LA. Among the prepared leakproof composites, LA/RC-4060 displayed the highest energy storage capacity with latent heat values of 64.2 J/g for melting and 66.0 J/g for crystallization. The phase change temperatures were also found to be 43.46 °C during melting and 41.77 °C during solidifying. Moreover, LA/RC-4060 composite has good thermal reliability after 100 thermal cycles. LA/RC-4060 was modified with 5 wt% highly conductive expanded graphite (EP) particles, and the heat storage and release rate was significantly improved. Both of the composites displayed good thermal stability, while the presence of EP did not adversely affect the thermal storage characteristics of LA/RC-4060 composite. The analysis results highlight the potential of RC supported LA based composite PCMs for thermal energy storage applications and it resulted that the obtained form-stable composites are possible candidates for energy storage applications such as solar energy storage and thermoregulation of buildings with promising latent heat capacity, leakage resistance, and thermal reliability over 100 cycles. However, further investigations and analysis fully require their long-term performance under real operating conditions.

CRediT authorship contribution statement

Yasemin Erben: Investigation. **Hatice Hande Mert:** Writing – review & editing, Writing – original draft, Visualization, Methodology, Investigation, Conceptualization. **Mehmet Selçuk Mert:** Writing – review & editing, Writing – original draft, Visualization, Methodology, Investigation, Conceptualization.

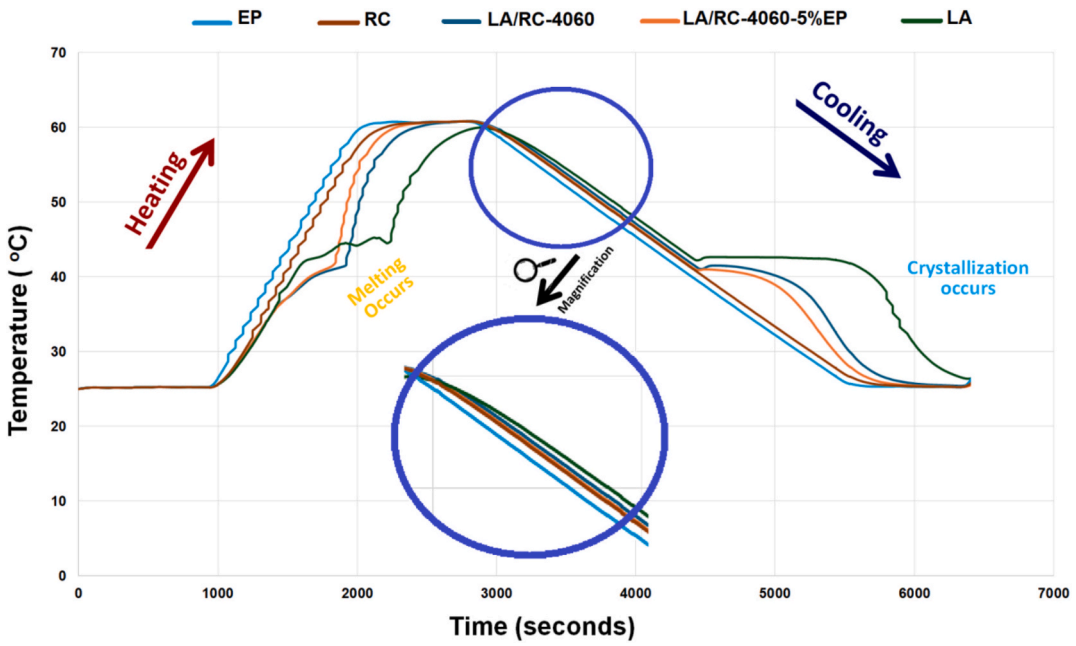

Fig. 13. Thermal behavior of the samples in the course of heating and cooling processes.

Table 7
Calculated heat storage rates of the samples in the course of cooling.

Observation	LA	EP	RC	LA/RC-4060	LA/RC-4060-%5 EP
Heat Storage Rate (∘C/s) – cooling	0.01098	0.01344	0.01271	0.01248	0.01272
Percentage of increment (%)	–	–	–	13.66%	15.85%

Declaration of competing interest

The authors declare that they have no known competing financial interests or personal relationships that could have appeared to influence the work reported in this paper.

Acknowledgment

This study was supported by Yalova University Scientific Projects Coordination Unit (Project No 2023/YL/0012).

Data availability

Data will be made available on request.

References

[1] Q. Zhang, J. Liu, J. Zhang, L. Lin, J. Shi, A Review of Composite phase Change Materials based on Biomass Materials, Polymers 14 (2022) 4089, https://doi.org/10.3390/polym14194089.
[2] M.S. Mert, H.H. Mert, The thermal Energy Storage Characteristics of Oleic Acid Modified ZnO-Decorated Polymer Matrix-Supported Composite phase Change Materials: Synthesis and Characterization, Macromol. Mater. Eng. (2024) 2400156, https://doi.org/10.1002/mame.202400156.
[3] P. Singh, R.K. Sharma, A.K. Ansu, R. Goyal, A. Sarı, V.V. Tyagi, A comprehensive review on development of eutectic organic phase change materials and their composites for low and medium range thermal energy storage applications, Sol. Energy Mater. Sol. Cells 223 (2021) 110955, https://doi.org/10.1016/j.solmat.2020.110955.
[4] S. Liu, J. Han, L. Wang, Y. Gao, H. Sun, W. Li, A lauric acid-hybridized bentonite composite phase-changing material for thermal energy storage, RSC Adv. 10 (43) (2020) 25864–25873.
[5] M. Ren, H. Zhao, X. Gao, Effect of modified diatomite based shape-stabilized phase change materials on multiphysics characteristics of thermal storage mortar, Energy 241 (2022) 122823.
[6] Z. Fan, Y. Zhao, Y. Ding, Y. Shi, X. Liu, D. Jiang, Fabrication and comprehensive analysis of expanded perlite impregnated with myristic acid-based phase change materials as composite materials for building thermal management, J. Storage Mater. 55 (2022) 105710.
[7] Z. Fan, Y. Zhao, X. Liu, Y. Shi, D. Jiang, Development of a new composite material for building energy storage based on lauric acid-palmitic acid-paraffin ternary eutectic and expanded perlite, J. Storage Mater. 53 (2022) 105136.
[8] Y. He, X. Zhang, Y. Zhang, Q. Song, X. Liao, Utilization of lauric acid-myristic acid/expanded graphite phase change materials to improve thermal properties of cement mortar, Energ. Buildings 133 (2016) 547–558.
[9] X. Liu, Y. Zhao, Z. Fan, Y. Shi, D. Jiang, Preparation and characterization of lauric acid–stearic acid/expanded perlite as a composite phase change material, RSC Adv. 12 (37) (2022) 23860–23868.
[10] N. Kumar, P.K.S. Rathore, R.K. Sharma, N.K. Gupta, Integration of lauric acid/zeolite/graphite as shape stabilized composite phase change material in gypsum for enhanced thermal energy storage in buildings, Appl. Therm. Eng. 224 (2023) 120088.
[11] Mehmet Selçuk Mert, Hatice Hande Mert, Müslüm Arıcı, Development and properties of n-octadecane / kaolinite composites as form-stabilized phase change materials for energy storage, J. Clean. Prod. 410 (2023) 137304, https://doi.org/10.1016/j.jclepro.2023.137304.
[12] P. Singh, R.K. Sharma, M. Khalid, R. Goyal, A. Sarı, V.V. Tyagi, Evaluation of carbon based-supporting materials for developing form-stable organic phase change materials for thermal energy storage: a review, Sol. Energy Mater. Sol. Cells 246 (2022) 111896, https://doi.org/10.1016/j.solmat.2022.111896.
[13] V. Voronin, D., Ivanov, E., Gushchin, P., Fakhrullin, R., & Vinokurov, V., Clay composites for thermal energy storage: a review, Molecules 25 (7) (2020) 1504.
[14] P.K.S. Rathore, S.K. Shukla, Enhanced thermophysical properties of organic PCM through shape stabilization for thermal energy storage in buildings: a state of the art review, Energ. Buildings 236 (2021) 110799.
[15] M.M. Umair, Y. Zhang, K. Iqbal, S. Zhang, B. Tang, Novel strategies and supporting materials applied to shape-stabilize organic phase change materials for thermal energy storage–a review, Appl. Energy 235 (2019) 846–873.
[16] Z. Zhan, L. Lin, J. Zhang, Z. Li, Q. Zhang, Q. Wang, Effect of In Situ Polymerization on the thermal Stability and Enthalpy Properties of Wood-Based Composites based on Graphene Oxide–Modified phase Change Microcapsule, Polym. Compos. (2025).
[17] Y. Chen, W. Wang, G. Fang, Thermal performance of lauric acid/bentonite/carbon nanofiber composite phase-change materials for heat storage, J. Mater. Eng. Perform. 33 (1) (2024) 348–361.
[18] S. Liu, S. Xin, S. Jiang, Study of Capric–Palmitic Acid/Clay Minerals as Form-Stable Composite Phase-Change Materials for thermal Energy Storage, ACS Omega 6 (49) (2021) 34192.
[19] M.G. Ali, H. Hassan, K. Thu, T. Miyazaki, S.A. Nada, Energy and economic evaluation of thermal regulation of PV panels using a hybrid phase change material-evaporative clay cooling system, Appl. Therm. Eng. 127600 (2025).
[20] H. Guo, Q. Sun, C. Yuan, X. Li, Y. Zhao, Experimental investigation on the physical and mechanical properties of silty clay enhanced by microencapsulated phase change materials, Case Stud. Constr. Mater. 20 (2024) e03151.

[21] H. Guo, Q. Sun, C. Yuan, X. Li, J. Wang, C. Sun, Study on the effect of deformation and strength characteristics of microencapsulated phase change materials on modified silty clay under dry and wet cycles, Constr. Build. Mater. 441 (2024) 137548.
[22] Z. Guo, J. Qiao, X. Liu, F. Lin, M. Liu, M. Fang, X. Min, Advances in mineral-based composite phase change materials for energy storage: a review, Green and Smart Mining Engineering, 2024.
[23] C.M. Stevenson, M. Gurnick, Structural collapse in kaolinite, montmorillonite and illite clay and its role in the ceramic rehydroxylation dating of low-fired earthenware, J. Archaeol. Sci. 69 (2016) 54–63.
[24] L.H. Rabelo, R.A. Munhoz, J. Marini, S.C. Maestrelli, Development and Characterization of PLA Composites with High Contents of a Brazilian Refractory Clay and improved Fire Performance, Mater. Res. 25 (2022) e20210444, https://doi.org/10.1590/1980-5373-MR-2021-0444.
[25] S. Liu, J. Han, Q. Gao, W. Kang, R. Ren, L. Wang, D. Wu, Lauric acid/bentonite/flake graphite composite as form-stable phase change materials for thermal energy storage, Mater. Express 10 (2) (2020) 214–224.
[26] A.H. Alkhazaleh, W. Almanaseer, A. Alkhazali, Experimental investigation on thermal properties and fire performance of lauric acid/diphenyl phosphate/expanded perlite as a flame retardant phase change material for latent heat storage applications, Sustainable Energy Technol. Assess. 56 (2023) 103059.
[27] B. Kekevi, H.H. Mert, M.S. Mert, E.H. Mert, Preparation and characterization of palmitic acid/polymer composite phase change materials supported with cross-linked poly (limonene-co-ethylene glycol dimethacrylate) copolymers for low-temperature thermal applications, React. Funct. Polym. 198 (2024) 105884.
[28] Louati, S., Baklouti, S., & Samet, B. (2016). Geopolymers Based on Phosphoric Acid and Illito-Kaolinitic Clay. *Advances in Materials Science and Engineering*, *2016*(1), 2359759.
[29] Rezende, J. C. T., Ramos, V. H. S., Oliveira, H. A., Oliveira, R. M. P. B., & Jesus, E. (2018, February). Removal of Cr (VI) from aqueous solutions using clay from Calumbi geological formation, N. Sra. Socorro, SE State, Brazil. In *Materials Science Forum* (Vol. 912, pp. 1-6). Trans Tech Publications Ltd.
[30] B. Li, T. Liu, L. Hu, Y. Wang, L. Gao, Fabrication and properties of microencapsulated paraffin@ SiO2 phase change composite for thermal energy storage, ACS Sustain. Chem. Eng. 1 (3) (2013) 374–380, https://doi.org/10.1021/sc300082m.
[31] X. Hou, Q. Li, Z. Yang, Y. Zhang, W. Zhang, J.J. Wang, Temperature–humidity dual regulation of a single-core–double-shell microcapsule fabricated by electrostatic-assembly and chemical precipitation, RSC Adv. 10 (44) (2020) 26494–26503, https://doi.org/10.1039/D0RA03554H.
[32] X. Huang, X. Chen, A. Li, D. Atinafu, H. Gao, W. Dong, G. Wang, Shape-stabilized phase change materials based on porous supports for thermal energy storage applications, Chem. Eng. J. 356 (2019) 641–661.
[33] C. Cárdenas-Ramírez, M.A. Gómez, F. Jaramillo, A.G. Fernández, L.F. Cabeza, Experimental determination of thermal conductivity of fatty acid binary mixtures and their shape-stabilized composites, Renew. Energy 175 (2021) 1167–1173.
[34] Y. Yuan, N. Zhang, T. Li, X. Cao, W. Long, Thermal performance enhancement of palmitic-stearic acid by adding graphene nanoplatelets and expanded graphite for thermal energy storage: a comparative study, Energy 97 (2016) 488–497, https://doi.org/10.1016/j.energy.2015.12.115.
[35] S. Liu, H. Yang, Composite of Coal-Series Kaolinite and Capric–Lauric Acid as Form-Stable Phase-Change Material, Energ. Technol. 3 (1) (2015) 77–83.
[36] P. Liu, X. Gu, J. Rao, S. Liu, B. Wang, L. Bian, Preparation and thermal properties of lauric acid/raw fly ash/carbon nanotubes composite as phase change material for thermal energy storage, Fullerenes, Nanotubes, Carbon Nanostruct. 28 (11) (2020) 934–944.
[37] G. Hekimoğlu, M. Nas, M. Ouikhalfan, A. Sarı, Ş. Kurbetci, V.V. Tyagi, T.A. Saleh, Thermal management performance and mechanical properties of a novel cementitious composite containing fly ash/lauric acid-myristic acid as form-stable phase change material, Constr. Build. Mater. 274 (2021) 122105.
[38] R. Wen, X. Zhu, C. Yang, Z. Sun, L. Zhang, Y. Xu, Z. Huang, A novel composite phase change material from lauric acid, nano-Cu and attapulgite: Preparation, characterization and thermal conductivity enhancement, J. Storage Mater. 46 (2022) 103921.